The influence of the experimental span of Time-resolved X-ray tomography on dynamic parameters in a fluidized bed

C. Rautenbach[1], R. F. Mudde[3], M. C. Melaaen[1,2], B. M. Halvorsen[1,2]
[1]Department of Process, Energy and Environmental Technology, Telemark
University College, Porsgrunn, Norway.
[2]Telemark R & D Centre (Tel-Tek), Porsgrunn, Norway.
[3]Kramers Laboratorium voor Fysische Technologie, Delft University of Technology,
Delft, The Netherlands

Keywords: Fluidization, X-ray tomography, Experimental-span, Bubbles size, velocity and frequency

Abstract — Fluidized beds have presented some problems to experimentalists in the past due to their opaque nature [1]. This problem has however been overcome by non-intrusive nor invasive measurement techniques. X-rays or Gamma rays can move through such systems where light (low energy radiation) cannot. Tomographic techniques can thus also be used with nuclear methods and is generally referred to as nuclear densitometry [1].

Using Time-resolved X-ray tomography on a fluidized bed is a state of the art technique. The first data of such a system has been presented by [1]. With this technique being novel, a thorough investigation of the measurement scenarios has not been performed thus far. The current study will focus on the influence of the experimental span on the average bubble velocity, bubble frequency and bubble volume. The influence of thresholding was investigated and the accuracy of the obtained results will be determined by existing empirical equations. In all of the experiments, glass particles were used with a particle size distribution of 79-149 μm.

In the present study the bed was fluidized using a single central jet and a porous plate distributer. This experimental set-up was chosen to make the study of the dynamic parameters more reliable and to include the uncertainties associated with a freely bubbling bed. The measurement technique is briefly discussed and it is concluded that at least 45 s is required to obtained a reliable result for the bubble velocity in a freely bubbling bed while at least 25 s are required to obtain reliable results for the bubble volume and frequency.

INTRODUCTION

Fluidized bed reactors are currently being used in a wide range of industrial applications. Some applications are still in development (like Chemical Looping Combustion (CLC)) and others have been used successfully for decades (for example catalytic reactors). The development of state of the art measuring techniques helps researchers to understand the complex multiphase flow behaviour of fluidized beds and thus enables the research community to better design and utilize fluidized bed technology. One such state of the art measuring technique is Time-resolved X-ray tomography.

Currently there are several tomographic systems being used in process technological research. These systems include Electrical Capacitance Tomography (ECT), Electrical Resistance Tomography (ERT) and X-ray Tomography. Using these measuring techniques an opaque

system, like a fluidized bed, can become transparent [1]. X-rays, Gamma rays, Electrical fields and current can move through such systems where light (low energy radiation) cannot. Tomographic techniques can thus also be used with nuclear methods and is generally referred to as nuclear densitometry [1]. Techniques like ECT and Electrical Impedance Tomography (EIT) operates with soft fields. These soft field techniques operates on the principal that a change in the electromagnetic field at one location influences the entire field [1]. The draw back of such techniques is typically that the size of the experimental tower is limited.

Nuclear tomographic techniques or nuclear densitometry relies on hard fields and does not have the same sort of constraints the soft field measuring systems have. An example of a hard field measuring technique is X-ray tomography. Thus larger tower diameters can be studied without the loss of resolution in the center of the tower. These nuclear measuring techniques have the added disadvantage of being dangerous and expensive compared to other techniques. Special lead insulated room or facilities are required together with advance safety protocols and regulations. There is always some inherent noise associated with nuclear techniques and because of this the temporal resolution is relatively low compare to some of the other tomographic modalities [1].

The time-resolved X-ray tomography system used in the present study is located at the Technical University of Delft (TU Delft) in the Netherlands. The measurements obtained using this system together with Digital Image Processing (DIP) package produced by the Quantitative Imaging Group from TU Delft, made it possible to create 3D images of bubbles encountered in a fluidized bed. These 3D images also provide information about the recorded bubbles, such as the bubble volume, frequency and location. In Figure 1 (a) a typical 3D image is provided collected over a 1.6 s time interval. In Figure 1 (b) an image is provided before it was processed into a three dimensional form. These 2D images are staked to create the 3D image shown in Figure 1 (a).
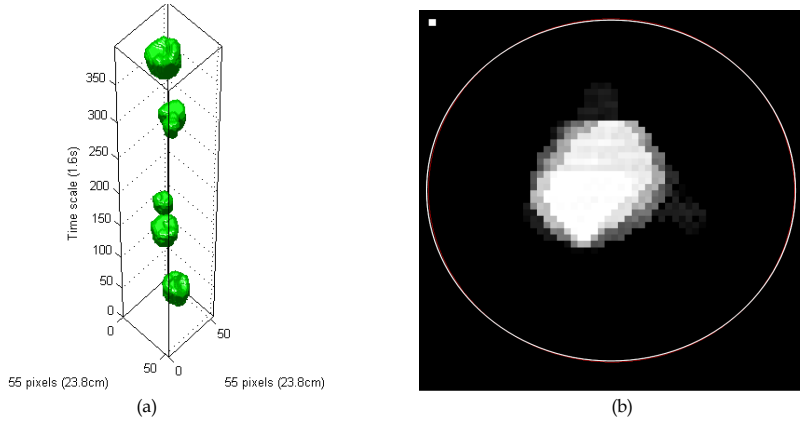

(a)   (b)

Figure 1: (a) 3D-image of bubbles rising in a fluidized bed with a 55×55 pixel resolution. (b) A typical 2D grayscale 'slice' image of a bubble rising in a fluidized bed. The white line indicates the experimental tower and at the top left corner the size of a single pixel is illustrated.

To be confident in the results obtained from the time-resolved X-ray tomography system it is important to investigate several measuring scenarios and the reliability of the results under typical operating conditions [3]. This was done in the present study with the focus on the experimental span and its influence on the dynamic parameters of a fluidized bed.

EXPERIMENTAL PROCEDURE

Experimental Setup

In the measurement system used in the present study three X-ray sources were used that each created a fan beam through the fluidized bed. Each fan beam fell onto two array detector

consisting of 32 CdWO$_4$ detectors [1]. The set-up used in the present study is illustrated in Figure 2. The red lines represent the path of radiation detected by each detector respectively. The fluidized bed is located in the middle of the set-up, surrounded by the detectors and sources and its diameter was 23.8 cm. Figure 2 was created by a simulation program developed by Mudde and co-workers at TU Delft.
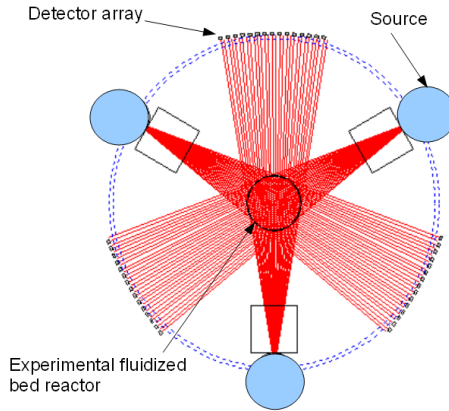

Figure 2: Three X-ray sources that simultaneously radiate an X-ray fan beam through the experimental fluidized bed tower or reactor. Two sets of 32 detectors have been allocated to each source.

The X-ray system can have a sampling frequency of 2500 frames/s but due to some inherent noise in the X-ray sources the obtained data had to be averaged. This was done by averaging over ten measurements which in turn lowered the sampling frequency to 250 frames/s. This averaged data can be converted to a line-averaged solid fraction value by using calibration curves [1].

The TU Delft X-ray tomography system consists of two arrays of detectors 4 cm apart and both consisting of 32 detectors for each of the 3 sources. The distance from the center of the bed to the detector arrays was 85.8 cm and the distance from the center of the bed to the sources was 71.6 cm. All of the X-ray beams originate from an approximate point source and diverges from there. Thus the effective distance between the measuring planes can be shown to be equal to 1.86 cm . With these two measuring planes it was possible to determine the bubble rise velocity. Bubble size and velocity are crucial in determining factor such as the particle residence time, particle entrainment and heat and mass transfer in a fluidized bed [2]. Thus to be able to determine the bubble shape, size and velocity is of paramount importance and the X-ray tomographic system allows researchers to do exactly that.

All the experiments were carried out with a 79-149 µm glass powder that produced a solid fraction value of 0.66 in the packed bed (non-fluidized) state. The experimental tower was made from plexi-glass and ambient air was fed into the bed by either a single jet or via a porous plate distributor. The jet was used as a validation method together with hollow plastic cylinders of different sizes. Measurements of these two scenarios produce predictable results and are a good way to test the system before dealing with the uncertainties associated with freely bubbling beds.

In Figure 3 the experimental tower used in the present study is illustrated. For the experiments done with the single jet the air was not fed through the porous plate and vice versa. During the investigation two different sizes of plastic cylinders (we shall call the phantoms) were inserted at several locations within the fluidized bed. It was found that the resolution in the center of the bed was worse than at the area close to the walls. The explanation for this

phenomena lies within the high attenuation of the glass particles. Because the center beams have to pass through a lot of material close to the center of the bed, more radiation is attenuated, compared to the short path length attenuation close to the tower walls.
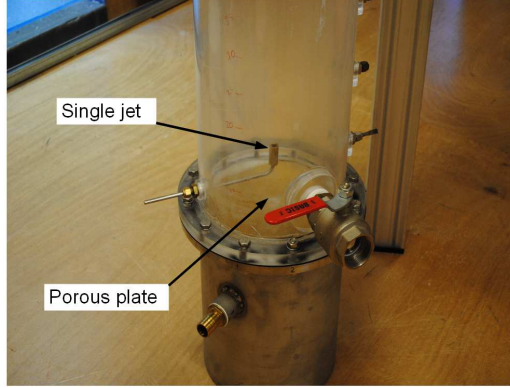

Figure 3: Experimental tower used in the present study equipped with a single jet and a porous plat distributer.

The radiation levels can readily be increased to 'see' more in the center of the bed but this will lead to the very real possibility of over exposing the detectors aligned with the short path lengths. The solution could be to place copper plates in front of the side detector in unison with increasing X-ray energy. Unfortunately this solution has not yet been applied for the present work and thus the spatial resolution at the center of the tower is just above 2.5 cm.

Calibration

Each detector measures the attenuation of a small cone shaped beam coming from the X-ray source located on the opposite side of the fluidized bed. This small cone is approximated as a line and treated as such in the reconstruction [1]. For mono-energetic gamma- or X-rays passing through a fluidized bed, the number of photons registered per second in a single approximated line will follow the Lambert-Beer law which states that

$$R = R_0 \exp\big(1\big(\phi_s \mu_p + (1 - \phi_s)\mu_g\big)d_t\big),$$ (1)

where R_o is the number of photons detected per second in a vacuum including the fluidized bed wall, ϕ_s is the solid fraction and μ_p and μ_g is the linear absorption coefficient for the solid and gas phase respectively. d_t is the inner diameter of the fluidized bed tower [1].

For a mono-energetic source a two point calibration would be sufficient. This would be calibration much like that of an ECT system with an empty tower and a full tower of particles. Most X-ray sources produce a wide spectrum of X-ray energies and thus a two point calibration is not adequate [1]. This implies that μ is a function of the photon energy E. Non-linearity is also obtained due to the fact that the low energy photos are absorbed much faster than high energy photons. Hence, R (measured number of photons) does not follow the Lambert-Beer law [1]. During calibration the effect of 'beam hardening' has to be accounted for. Beam hardening occurs as an increasing amount of powder is present on a particular X-ray beam and the relative number of high-energy photos increases [1]. To account for this effect each detector is calibrated individually with several amounts of powder. Seven calibration points are usually used in total including an empty and full tower as the two extreme values [1]. In the current study a five point calibration has been used due to the high attenuation of glass particles in comparison to that of polystyrene particles. If seven points were used, including an empty bed, the radiation

would have been to low to get meaningful measurements. Our calibration thus entailed the center beams passing through 1/3, 1/2, 2/3, 5/6 of a full bed and a full bed. Using these calibration points the radiation level could be set high enough as to obtain meaningful measurements but also low enough as to not over expose the detector and thus avoid the detector from clipping. These criteria were chosen under the assumption that there won't be any bubbles, during the course of the experiments, with an effective diameter much greater than 2/3 of the tower diameter.

In Figure 4 (a) an example of a calibration curve is provided. A calibration curve was produced for each detector of all three double plane detector arrays. For each calibration curve three constants were determined, namely: A_{cal}, B_{cal} and C_{cal}. These constants determined the calibration curve of the form

$$A_{cal} + B_{cal} \times \exp(-x/C_{cal}) \, , \qquad (2)$$

where x is the path length of a particular beam through the particles aligned with a particular detector [1]. This exponential curve is also illustrated in Figure 4 (a) and its only purpose is to provide a relationship between particle path length and measured attenuation. It is important to remember that the attenuation of the radiation is only a function of the amount of powder on its path [1]. In calculating these calibration values 5 s of measured attenuation values were collected for each detector array. Then these 1250 values were averaged for each detector to produce the representative measured attenuation values for each detector and for each calibration point.

Before the actual measurements were made a segment of data were taken where no bubbles were present and it was then compared to the full undisturbed bed data obtained from calibration. In theory the ratio of these averaged detectors measured attenuations should be equal to 1 if the calibration is working properly. In Figure 4 (b) it is clear that this was not the case.
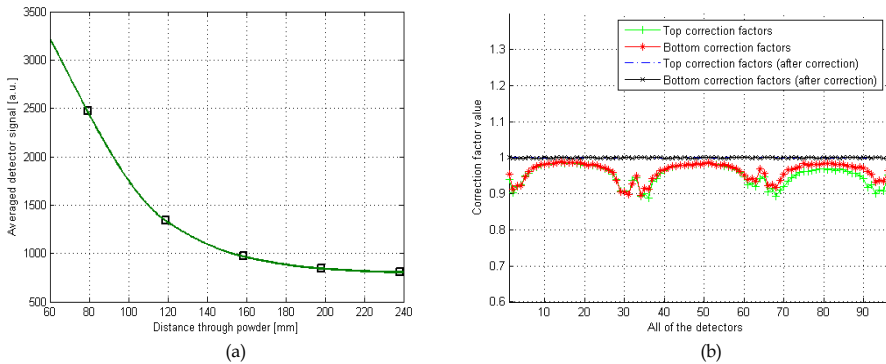

Figure 4: (a) An example of 5 calibration points for the 16th detector of one of the three top detector arrays. (b) Correction factors for all of the detectors (3×32 detectors) before and after applying the correction factor.

From Figure 4 (b) it is clear that for each of the three detector arrays a near parabolic-shaped discrepancy is obtained. This might be due to the motion of particles in the fluidized bed after fluidization and the consequent redistribution of particles. The powder used in the present study has a large particle size distribution and thus a non-uniform particle distribution can be expected and was observed in the actual experiments. The correction factors obtained in Figure 4 (b) were used to correct all the collected data to account for these effects associated with the fluidization of the bed. In Figure 4 (b) the same ratios are also shown after it has been corrected with the correction factors.

RESULTS AND DISCUSSION

Thresholding

As part of the measurement scenario of most tomographic measurements in fluidized beds, a threshold has to be assigned to define the bubble size. The threshold value can range from 0 to 1 and the closer the value is to 0 the bigger the measured bubble will be (refer to Figure 1 (b) where a typical greyscale image was illustrated with 1 indicating white and 0 black). To get a reliable value of the threshold value the phantoms could be used as these cylindrical objects had a known diameter and thus the threshold could be adjusted accordingly. Although this should be quite reliable the plastic wall of the phantom might create a situation that is not representative of the actual fluidized bed bubbles.

Thus instead of using the phantoms, a predictive correlation was used to estimate the average bubble size. According to a literature review done by Karimipour and Pugsley [2] the most reliable correlation for bubble size prediction of Geldart **B** particles are given by Choi et al. and the trivial correlation of Mori and Wen [2]. The performance of the correlations investigated by Karimipour and Pugsley were quantified by calculating the squared difference between the correlation prediction and experimental values collected from several published results [2]. The equation by Mori and Wen was used in the present study due to its simplicity and prediction accuracy and is given as

$$\frac{d_{bm} - d_b}{d_{bm} - d_{b0}} = e^{-0.3z/d_t} \quad [\text{cm}], \tag{3}$$

where d_{b0} is the initial bubble size formed near the bottom of a bed supported by a porous or perforated plate distributer [2, 4]. d_b is the equivalent diameter calculated from a sphere with the same volume as the average bubble volume of a particular experiment, z is the bed height at which the measurements are taken and d_t is the experimental tower diameter. d_{bm} is known as the limiting bubble size in a very deep bed and is expressed as

$$d_{bm} = 0.65\left(\frac{\pi}{4}d_t^2\left(u_0 - u_{mf}\right)\right)^{0.4} \quad [\text{cm}], \tag{4}$$

with u_0 the superficial velocity and u_{mf} the minimum fluidization velocity [4]. The range of conditions from which equation (4) was formulated contains the present study. According to Karimipour and Pugsley [2] the equation most researcher use to estimate the initial bubble size, d_{b0}, formed near a porous plate distributer is given by Miwa et al. and is expressed as

$$d_{b0} = 0.00376\left(u_0 - u_{mf}\right)^2 \quad [\text{cm}]. \tag{5}$$

Given that the measurements were taken at a height of 46.2 cm in the fluidized bed and that $u_0 - u_{mf} = 5.1$ cm/s, a bubble size of 6.4 cm was predicted. Using 50 s of data collected with an experiment conducted under the same operating conditions and using a porous plate distributer the average bubble volume could be calculated. Then the threshold value was changed until an average bubble volume was obtained that produce an equivalent diameter approximately equal to 6.4 cm. A threshold value of 0.465 was found to accomplish this and was then used as the threshold value for the remainder of the experiments.

Experimental span

Previous research performed with other tomography modalities suggests a strong dependence on the experimental span [3]. Makkawi and Wright investigated the experimental span over a whole range of different operating condition using an ECT system [3]. According to their literature study there was no thorough investigation into a measurement scenario for an ECT system prior to their research. Because of this reported strong dependence of the dynamic parameters on the experimental span for the ECT system, a thorough investigation regarding the dependence of the bubble velocity, volume and frequency on the experimental span for the time-resolved X-ray tomography system was performed in the present study. The present study will provide future researchers a guide for planning and designing a reliable experimental measuring scenario using the time-resolved X-ray tomography system.

Influence of the experimental span on the average bubble velocity

The bubble velocities were determined by using the two planes of the X-ray system. Using the two planes, with a known distance between them, it was possible to trace the bubbles from one plane to the next and thus measure the time it took for a particular bubble to ascend from the lower plane to the top plane. An example of the range of bubble velocities recorded in a single experiment is provided in Figure 5. This data was obtained with a freely bubbling bed using a porous plate distributer. The data was recorded over a 50 s period and this time limit will form the maximum experimental time span in the present study.
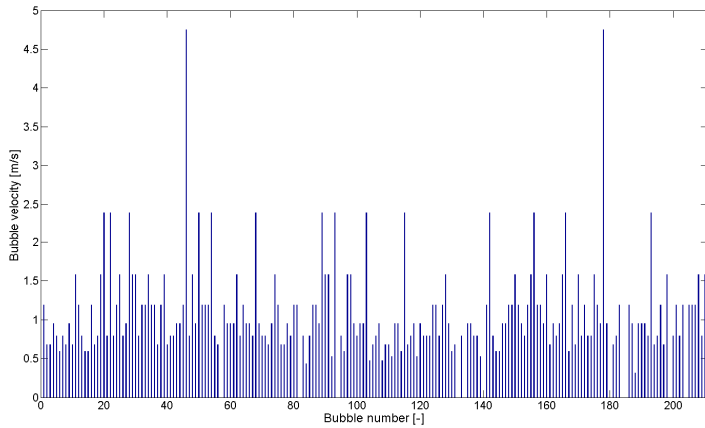

Figure 5: Example of bubbles recorded during a 50 s experimental run together with their measured bubble velocities. For this experimental scenario $u_0 - u_{mf} = 5$ cm/s.

The average bubble velocity over the particular experimental span will be used to investigate the influence of the experimental span on the bubble velocity. In Figure 6 the bubble rise velocity is given as a function of the experimental span for both fluidization via a single jet and via a porous plate distributer.

From Figure 6 (a) it is clear that the bubble rise velocity for a single jet remains nearly constant after 40 s with an error less than 5 %. Thus it seems safe to conclude that the bubble rise velocity of a single jet can be reliably determined after an experimental span of only 40 s. The same could not be concluded from Figure 6 (b) where the bed was fluidized via a porous plate distributor. With this freely bubbling bed at least 45 s was required to obtain a reliable result with an error less than 8 %. Although the bubble velocities in Figure 6 (b) stabilized after 45 s the values obtained for the excess velocity equal to 3.6 cm/s were higher than the values obtained with the 4.3 cm/s.
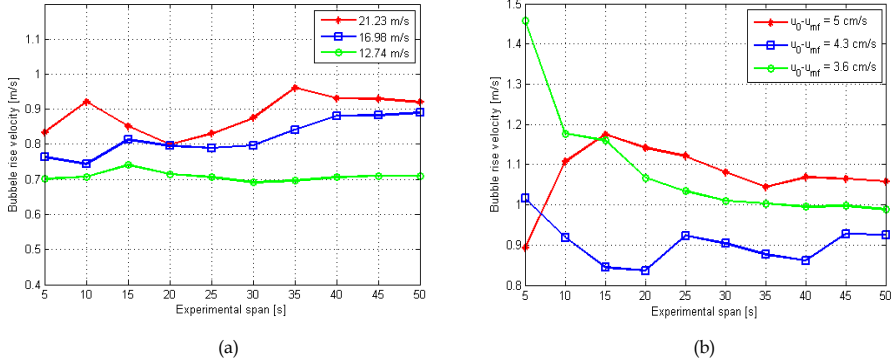
(a)

(b)

Figure 6: (a) The average bubble rise velocity computed over each experimental span for three different superficial jet velocities through a single jet at the bottom of the fluidized bed. (b) The bubble rise velocity as a function of the experimental span for three different excess gas velocities, fluidized via a porous plate distributer.

This is a highly counter intuitive result as smaller bubbles should rise slower according to most bubble velocity correlations. The explanation for the phenomena can be explained by mean of Figure 7.

In Figure 7 (a) the location of the bubble center is given in the form of the sample number at which it was recorded. The bubble volume is represented in pixels cubed (the unit before it is transformed into SI units). From Figure 7 (a) it is observed that the bottom plane data always supersedes the top plane data. This is trivially correct as the bubble must pass the bottom plane before it passes the top plane. The encircled data points indicate bubble that has been match as being the same bubble traversing from the bottom to the top plane. The problem can be observed in the data points that were not 'matched'. From visual observation of the reconstructed data it was concluded that some of the smaller bubbles were not reconstructed correctly and were in the range below the resolution of the current time-resolved X-ray tomography system. This could have caused the bubble rise velocity measurements to be bias towards the higher velocity bubbles.
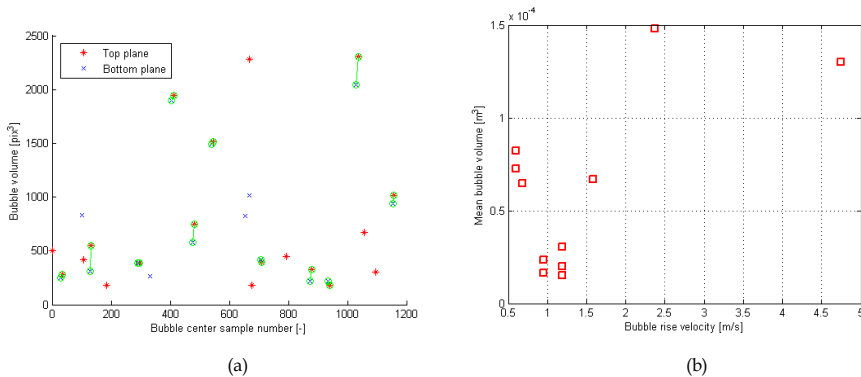

(a)

(b)

Figure 7: (a) Bubbles recorded during the first 5 s of the experiments done where the bed was fluidized through a porous plate with an excess gas velocity equal to 3.6 cm/s. The encircled data points indicate bubbles that matched from both the top and bottom plane. (b) Bubble volume as a function of the bubble rise velocity for the same 5 s experiment.

In Figure 7 (b) the bubble volume is given as a function of the bubble rise velocity. The bubble volume was calculated from taking the average volume between the bottom and the top plane.

From Figure 7 (b) it is clear that larger bubbles do not necessarily imply a larger bubble rise velocity although over an average this will be the expected result.

Influence of the experimental span on the average bubble volume

In Figure 8 the average bubble volume is given as a function of the experimental span. Both a jet and a porous plate were used and the results are provided. The volume of each bubble was computed with the bubble rise velocity of that particular bubble. The results obtained for the average bubble volume had a more stable behaviour over a shorter time in comparison to that of the bubble rise velocity. For the experiments done with the single jet, Figure 8 (a), an experimental span of 45 s produces results with less than 2 % error and for an experimental span of only 20 s an error of less than 6 % is achieved. Thus if 6 % error is adequate for a particular application an experimental span of 20 s can be used with a reliable result.

For the experiments done with the porous plate distributer, Figure 8 (b), an experimental span of 25 s produces errors less than 7 % for all the investigated cases.
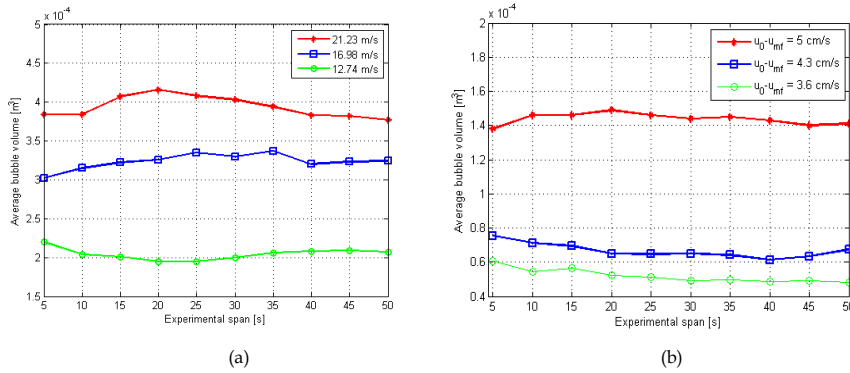

(a)   (b)

Figure 8: (a) The average bubble volume for three different superficial jet velocities through the single jet. (b) The average bubble volume for three different excess gas velocities through a porous plate distributer.

The data presented in Figure 6 and 8 were collected from the same experiments. Note that even though the average bubble volume in Figure 8 (b) decreased with a decreasing excess gas velocity the bubble rise velocity did not follow the same trend (as discussed previously using Figure 7).

Influence of the experimental span on the bubble frequency

In Figure 9 the bubble frequency as a function of the experimental span is provided for using both a single jet and a porous plate distributer. In the single jet experiment an experimental span of 20 s produced an error of only 4 % and with the porous plate distributer a 25 s run produced an error of 5 %.

Similar to the average bubble volume results the bubble frequency requires less time per experiment to reach a reliable result. In Figure 9 (a) the bubble frequencies with a 21.23 m/s superficial jet velocity were lower than the 16.98 m/s superficial jet velocity data. It is known that slug flow behaviour will have the effect of lower bubble rise velocities [4]. Thus it is not that surprising that the 21.23 m/s superficial jet velocity could have caused near slug flow conditions and thus had the effect of larger, less frequent, bubbles or slugs.
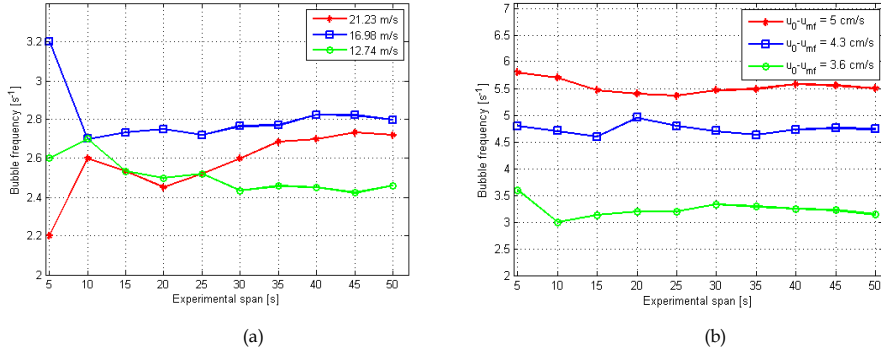
(a)   (b)

Figure 9: (a) The bubble frequency for three different superficial jet velocities using a single jet. (b) The bubble frequency for three different excess gas velocities using a porous plat distributer.

The largest bubble in the 21.23 m/s superficial jet velocity experiments reached a size of approximately 40 % of the tower diameter. The accepted size for a bubble to be classified as a slug is usually 50 % of the tower diameter [4].

CONCLUSIONS

Some dynamic parameters of a fluidized bed have been investigated as a function of the experimental span. These parameters were the bubble rise velocity, the average bubble volume and the bubble frequency. Several different superficial gas velocities were also used to investigate the effect of the experimental span on these particular dynamic parameters. In previous research done on this topic, but with an Electrical Capacitance Tomography system (ECT system), it was found that a minimum experimental span of 60 s must be used to obtain reliable results [3]. The dynamic parameters that [3] investigated were the bubble rise velocity and frequency. For measuring the solid fraction [3] found that 20 s will produce a reliable result.

For the time–resolved X-ray tomography system investigated in the present study different results were obtained. In using a single jet it was found that a measuring span of 40 s produced reliable results for the bubble rise velocity. In the case of the average bubble volume and bubble frequency a 20 s experiment produced reliable results with using the single jet. In using the porous plate distributor a measuring span of 45 s were adequate for determining the bubble rise velocity while 25 s were reliable enough for the average bubble volume and bubble frequency. From using empirical equations it was also estimated that a threshold value of 0.465 will produce result that most agree with previously estimated correlations.

The present study forms part of exploring the capabilities of the time-resolved X-ray tomography system and functions as a user manual for future researchers [3].

ACKNOWLEDGMENTS

REFERENCES

1. Mudde, R.F. 2010. Time-resolved X-ray tomography of a fluidized bed. *Powder Technology*. **199**:55–59.

2. Karimipour, S. & Pugsley, T. 2011. A critical evaluation of literature correlations for predicting bubble size and velocity in gas-solid fluidized beds. *Powder Technology.* **205**:1-14.

3. Makkawi, Y.T. & Wright, P.C. 2004. Electrical capacitance tomography for conventional fluidized bed measurements-remarks on the measuring technique. *Powder Technology.* **148**:142-157.

4. Kunii, D. & Levenspiel, O. 1977. *Fluidization Engineering*. Huntington, NY: Robert E. Krieger Publishing Company.

Errata

In Paper E there was a typo. Equation (1) should have been expressed as

$$R = R_0 \exp\left(-\left(\phi_s \mu_p + (1 - \phi_s)\mu_g\right) d_t\right).$$
(E.1)

The minus in the exponent was miss typed as a 1 in equation (1).

It might be useful to express the jet flow in terms of the superficial velocity. The single central jet had a diameter of $1cm$. Using this information the superficial velocity can be calculated if desired.